Optimization of photocatalytic degradation of naphthalene using nano-TiO$_2$/UV system: statistical analysis by a response surface methodology

Vahid Mahmoodi*, Javad Sargolzaei

Faculty of Engineering, Department of Chemical Engineering, Ferdowsi University of Mashhad, Mashhad, Iran
Tel./Fax: +98 511 8816840; email: vahid.mahmoodi@stu.um.ac.ir

ABSTRACT

In this study, the response surface methodology (RSM) was applied for modeling and optimization of photocatalytic degradation of naphthalene using TiO$_2$ nanoparticles in a batch slurry system. The effect of four independent parameters such as agitation speed (X_1), air flow rate (X_2), catalyst loading (X_3), UV light intensity (X_4), and their interactions was investigated. A quadratic model was qualified to predict the degradation percent of naphthalene in different conditions, consequently. The significance of independent variables and their interactions were evaluated by the analysis of variance (ANOVA). Evaluation of the *p*-value approved that the effect of interactions is not very significant and so interaction terms were removed from the initial model. In order to achieve the maximum degradation percent, the optimum conditions were obtained by mathematical and statistical methods. The results showed that the maximum degradation efficiency can be achieved at the optimum conditions: X_1 = 150 rpm, X_2 = 5 L/h, X_3 = 2.17 g/L, and X_4 = 18.67 W. The good agreement between the predictive and experimental results at the optimum point verified the model adequacy and validity of the obtained optimum conditions.

Keywords: Photocatalysis; TiO$_2$; Response surface methodology (RSM); Central composite design (CCD); Optimization

1. Introduction

Polycyclic aromatic hydrocarbons (PAHs) are highly toxic agents that cause genetic changes, congenital abnormalities, and cancer. So these contaminants have specific importance in terms of environment. Between PAHs, naphthalene is the most soluble and chemically stable in water [1]. Therefore, the removal of naphthalene from water and wastewater has recently become the subject of considerable interest due to more strict legislations introduced in many countries to control water pollution.

The most important methods for removing organic contaminants from wastewater include coagulation and adsorption [2], ultrafiltration [3], nanofiltration [4], and biological filtration [5]. Most of these methods act based on displacement, release and transport of contaminants and so do not completely eliminate pollutions.

In recent years, photocatalytic process has shown many advantages such as great degradation potential and low cost in removal of organic contaminants from wastewater [6]. Photocatalysis is based on the

*Corresponding author.

production of unstable species with high reactivity tendency (e.g. $H_2O_2, O_2^{\cdot-}$, OH$^\cdot$) on a semiconductor surface (most often TiO_2) to convert the resistant organic materials to the inert components (e.g. CO_2, H_2O, NO_3^-, phosphate, halide ions) [7–9]. Because of high chemical stability, high efficiency, low production cost, and high refractive index leading to a hiding power and whiteness, TiO_2 can be an appropriate photocatalyst for the photocatalytic process [10].

Mechanism of the photocatalytic degradation of naphthalene is described in previous studies. Theurich et al. demonstrated that during the photocatalytic process, naphthalene is converted to different intermediates e.g. couramine, cinnamic acid, phethalic acid, and 1,2-benzenedicarboxaldehyde [11]. Also, Ohno et al. confirmed that during the photocatalytic degradation of naphthalene, the main product is 2-formylcinnamaldehyde [12].

Some researchers studied the kinetics and effect of some operational parameters such as photocatalyst dosage, reaction time, temperature, and initial concentration of contaminant on the photocatalytic reaction efficiency [13–15]. Lair et al. verified that kinetics of naphthalene degradation is consistent with the Langmuir–Hinshelwood mechanism [13]. In addition, Montazerozohori et al. investigated the kinetics of Photocatalytic decolorization of ethyl orange at various buffer solutions using nano-TiO_2 and showed that the kinetics investigations are in agreement with pseudo-first-order reaction rate for dye degradation. Also, they showed that in large amounts of photocatalyst, decolorization efficiency of dye reduces due to increased opacity of the suspension [14]. Wu et al. studied the photocatalytic decomposition of basic dye (HF6 coral pink) by nano-sized TiO_2 suspension at different temperatures and demonstrated that the dye decomposition rate increases with the reaction temperature. They stated that a higher temperature will raise the reaction rate constant and cause a faster decomposition rate based on the Arrhenius equation [15].

Performing a process at optimum conditions has many advantages such as reduction of energy consumption and approaching the higher efficiency [16,17]. Also, Low efficiency is one of the important barriers against photocatalytic process industrialization [6]. In the literature, to the best knowledge of the authors, statistical analysis and optimization of photocatalytic degradation of naphthalene from wastewater have not been reported.

Based on the above-mentioned facts, the specific objectives of this study were: (1) To apply a four factor, five-level central composite experimental design (CCD) for maximizing naphthalene removal from aqueous solution by UV/nano TiO_2 system; (2)

To examine the effects of four independent variables (agitation speed (X_1), air flow rate (X_2), catalyst loading (X_3), UV light intensity (X_4), and their interactions on the naphthalene removal efficiency; and (3) To verify the validity of the proposed model by additional batch experiments conducted in the experimental area of the CCD.

2. Materials and methods

2.1. Materials

The photocatalyst was TiO_2 at anatase crystalline phase with greater than 99.5% purity (average primary particle size: 30 nm, specific surface area: 50 ± 5 m^2/g) that was purchased from US Research Nanomaterials Inc. Naphthalene with analytical grade was purchased from Merck and Millipore deionized water was used for dilution at 45℃. TiO_2 nanoparticles were analyzed using X-ray powder diffraction with model of XRD, Philips PW 1800. The morphology/structure of TiO_2 nanoparticles were obtained by scanning electron microscopy (SEM, Cambridge S-360) and Transmission electron microscopy (TEM, Philips CM120).

2.2. Photo reactor

The photocatalytic reactor system is schematically exhibited in Fig. 1. A magnetic stirrer was used to mix the solution at different intensities. The reactor was equipped with three 8 W UV lamps at 365 nm
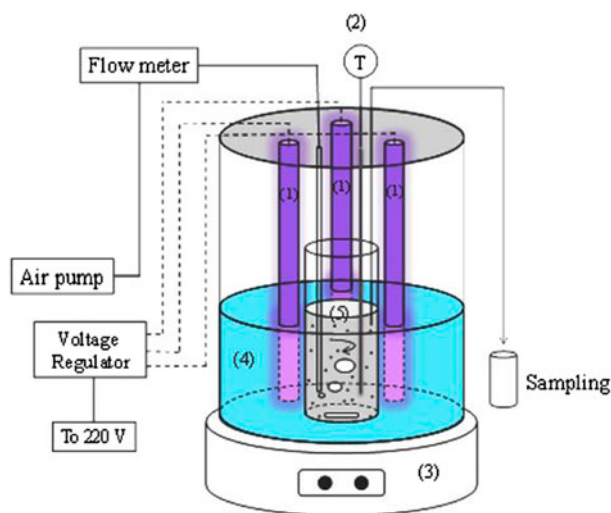
Fig. 1. Schematic diagram of the photocatalytic reactor system. 1—UV lamps; 2—Thermocouple; 3—Magnetic stirrer; 4—Water bath; 5—Suspension.

wavelength. The temperature was measured using a K-type thermocouple and was monitored by a temperature controller. An aquarium air pump was used for air injection into the solution weekly. Air flow rate was controlled using an accurate flow meter, and a water bath between the beaker and stainless steel container held the solution temperature constant during the experiment.

2.3. Procedure

First, 100 ml of naphthalene solution was poured inside a 150 ml beaker that was placed into a cylindrical stainless steel container. To reach thermal equilibrium, solution was stirred for 2 min extremely. In order to achieve the adsorption equilibrium, required amount of TiO_2 was added to the naphthalene solution and the suspension was stirred in darkness for 5 min. Then UV irradiation was started and the solution was sampled after 170 min. For separation of TiO_2 nanoparticles, the resulted samples were filtered by PTFE syringe membrane (0.45 μm pore size). Then samples were analyzed immediately by an UV/vis Spectrophotometer (CECIL 9000 series) at λ_{max} = 275.4 nm with a calibration curve based on the Beer–Lambert's law.

Fig. 2 presents the UV absorbance spectrum of the standard naphthalene solution at C_0 = 20 mg/L. The temperature of the solution was maintained at 32 ± 2°C during all the experimental test runs.

It is noteworthy that before performing the main tests, in a series of experiments in the dark, we realized that the adsorption equilibrium is attained after 5 min in the naphthalene/TiO_2/water system (Fig. 3).
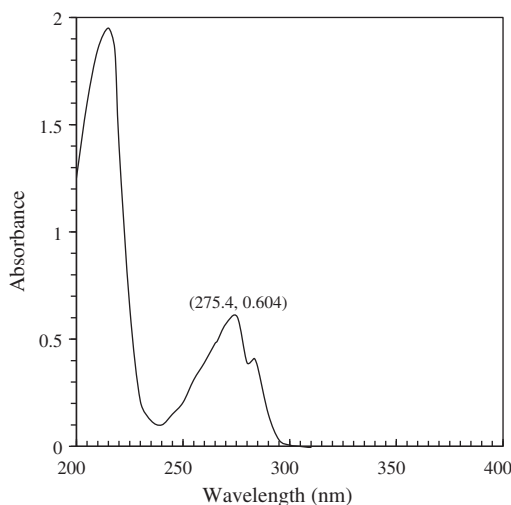
Fig. 2. UV absorbance spectrum of the naphthalene solution.
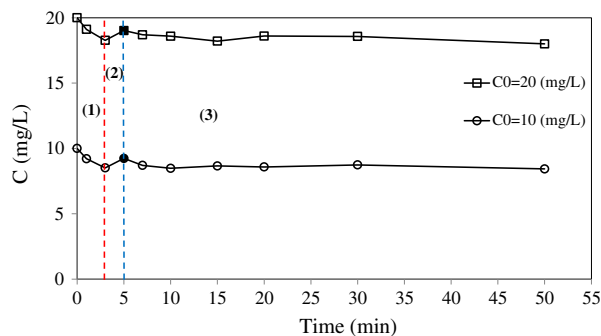
Fig. 3. Evolution of naphthalene adsorption on the TiO_2 surface in the dark, under the condition of X_1 = 100 rpm, X_2 = 0 L/h, and X_3 = 2 g/L.

As shown by Fig. 3, in the first moments, the TiO_2 showed considerable adsorption of the naphthalene (area 1). Then the naphthalene concentration increased slightly that may occur due to the partial desorption of naphthalene from the surface of TiO_2 (area 2). At area 3, the concentration stayed approximately constant and so it can be concluded that the adsorption has reached to the dynamic equilibrium after 5 min. Also, the results showed that less than 20% of the naphthalene was adsorbed on the surface of TiO_2 in the dark under specified conditions and no considerable degradation of naphthalene was observed without UV irradiation.

3. Response surface methodology (RSM)

In order to describe the effect of factors on the naphthalene degradation percent, a standard response surface method called orthogonal CCD with star points was employed with four factors and five levels. For statistical calculations, the variables X_i were coded as x_i according to the following equation:

$$x_i = \frac{X_i - X_0}{\Delta X} \qquad (1)$$

where x_i is the coded value of each independent variable, X_0 is the value of variable at the center point, and ΔX is the step change value [9]. The experimental ranges and levels of the independent variables for naphthalene removal are given in Table 1.

Also the experimental design as well as obtained output responses is shown in Table 2. In all experiments, the reaction time was equal to 170 min. The responses and corresponding parameters were analyzed and optimized using analysis of variance (ANOVA) to estimate the statistical parameters by means of statistical methods. Basically, this optimization process involves

Table 1
Experimental ranges and levels of the independent test variables ($\alpha = 2.0$)

Variables	Coded values				
	$-\alpha$	-1	0	$+1$	$+\alpha$
Agitation speed, X_1 [rpm]	0	50	100	150	200
Air flow rate, X_2 [L/h]	2	3	4	5	6
TiO$_2$ loading, X_3 [g/L]	1	1.5	2	2.5	3
UV light intensity, X_4 [W]	0	8	16	24	32

Table 2
CCD experiments, experimental and predicted values

Run No.	X_1 (rpm)	X_2 (L/h)	X_3 (g/L)	X_4 (W)	Degradation percent (%)	
					Experimental	Predicted
1	50	3	2.5	8	49.50	45.33
2	100	2	2.0	16	58.40	62.01
3	0.0	4	2.0	16	38.55	45.73
4	150	3	2.5	24	61.65	58.58
5	100	4	2.0	16	59.65	61.03
6	150	3	2.5	8	49.80	50.68
7	150	5	1.5	8	62.50	59.74
8	50	5	2.5	24	59.45	59.02
9	100	4	1.0	16	49.30	52.25
10	100	4	2.0	24	63.55	59.23
11	100	4	2.0	16	62.55	61.03
12	100	4	3.0	16	54.00	56.71
13	50	3	1.5	24	49.75	48.17
14	50	5	1.5	8	47.25	47.37
15	100	4	2.0	0	25.55	32.30
16	150	5	2.5	8	59.80	58.43
17	200	4	2.0	16	64.25	62.74
18	150	3	1.5	24	55.30	57.92
19	50	5	1.5	24	57.40	53.80
20	150	5	2.5	24	63.20	65.57
21	50	3	2.5	24	53.90	53.94
22	50	5	2.5	8	56.50	51.17
23	100	4	2.0	16	61.10	61.03
24	150	5	1.5	24	64.25	65.47
25	100	4	2.0	16	63.55	61.03
26	100	4	2.0	16	57.15	61.00
27	50	3	1.5	8	46.05	40.97
28	100	6	2.0	16	73.35	75.40
29	150	3	1.5	8	53.95	51.43
30	100	4	2.0	16	58.95	61.03

four major steps which are performing the designed experiments, estimating the model coefficients, predicting the response, and testing the fitness of the model [18].

The quadratic equation model for predicting the optimum conditions can be expressed according to the following relationship (Eq. (2)) [19]:

$$Y = \beta_0 + \sum_{i=1}^{k} \beta_i \cdot x_i + \sum_{i=1}^{k} \beta_{ii} \cdot x_i^2 + \sum_{i \leqslant j}^{k} \sum_{j}^{k} \beta_{ij} \cdot x_i \cdot x_j + \cdots + e \tag{2}$$

where Y is the response variable of degradation percent, β_0 the constant coefficient, β_i the linear coefficients, β_{ii} the quadratic coefficients, β_{ij} the interaction coefficients, x_i and x_j the coded values, k the number of factors in the experiment, and e is the random error. ANOVA was used for analysis of the data to obtain the interaction between the process variables and the responses. The quality of the fit polynomial model was described by the coefficient of determination (R^2) and model terms were evaluated by the p-value (probability) with 95% confidence interval. Three-dimensional plots and their corresponding contour plots were acquired for naphthalene degradation percent based on the effect of factors. Furthermore, the optimum conditions for attainment of maximum degradation percent were identified based on the main parameters. Design of experiments and statistical analysis was carried out with the assistance of Design Expert software[†].

4. Results and discussion

4.1. TiO$_2$ morphology and characteristics

As shown in Fig. 4, TiO$_2$ was analyzed by XRD which showed the presence of anatase as the nanoparticle crystalline phase.

TiO$_2$ nanoparticles were also analyzed by scanning electron microphotography (SEM) and Fig. 5 shows the morphology of the TiO$_2$ nanoparticles.

As seen in Fig. 5, the purity and porosity of TiO$_2$ nanoparticles are very appropriate. Also, Fig. 6 shows the transmission electron microscope (TEM) image of TiO$_2$.

Transmission electron microscopy could be the first method used to establish the size distribution of nanoparticles. Accordingly, Fig. 6 shows that the average particle size of pristine TiO$_2$ is less than 30 nm. This range of size can cause significant surface area and high degree of naphthalene degradation.

4.2. Model fitting and statistical analysis

After obtaining the initial model, evaluation of p-value parameter approved that the effect of interac-

---

[†]Vaughn, N.A., et al., Design Expert ®, version 8 for windows, Stat-Ease, Inc, Minneapolis, 2011, website: http://www.statease.com
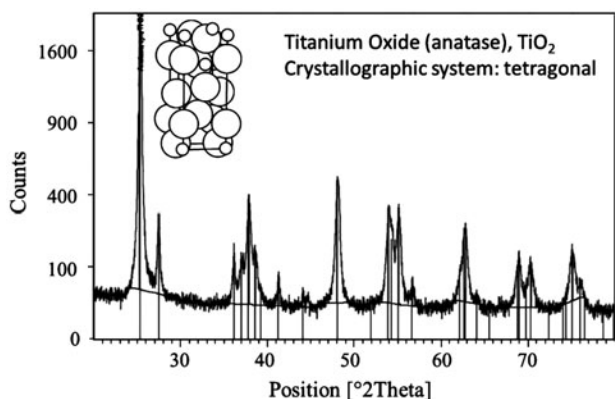
Fig. 4. X-ray diffraction pattern of the TiO_2 nanoparticles in anatase crystalline phase.
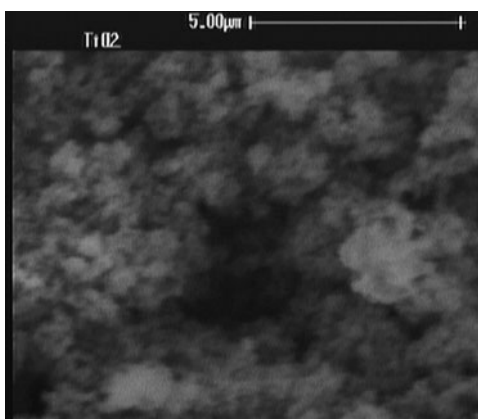
Fig. 5. SEM of the TiO_2 nanoparticles.
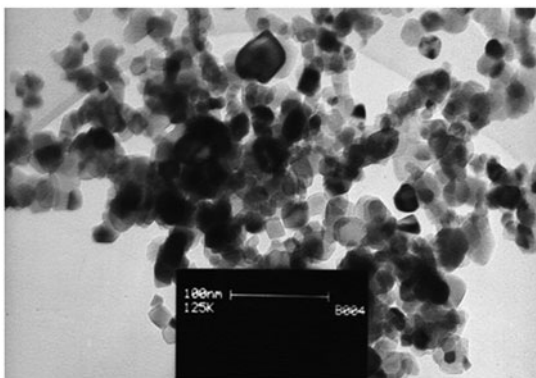
Fig. 6. TEM image of TiO_2 nanoparticles.

tions is not very significant (p-value greater than 0.05) and so interaction terms were removed from the initial model. According to the obtained results, coefficients

of the model were calculated by the following second-order polynomial equation in terms of coded values:

$$Y = 61.03 + 4.25\,x_1 + 3.35\,x_2 + 1.11\,x_3 + 3.59\,x_4 - 1.70\,x_1^2 + 1.92\,x_2^2 - 1.64\,x_3^2 - 5.39\,x_4^2$$

(3)

These results show that all independent variables at the first-order (linear term) state have positive effect on degradation efficiency and the most significant positive effect of the first-order derives from the agitation speed (x_1). Table 3 summarizes ANOVA for the modified quadratic response surface model consistent with experiments.

The quality of the fit of polynomial model was evaluated by the coefficient of determination R^2 and R^2adj, and statistical significance was checked by the F-test in the program. The Model F-value of 15.72 implies that the model is significant for naphthalene degradation. The p-values less than 0.0500 indicate that the model terms are also significant. As can be seen in Table 3, the coefficient of variance (CV) and adequate precision values for the naphthalene degradation percent were found to be 7.2 and 19.51, respectively. The CV value must be lesser than 10, otherwise the proposed model cannot be considered reproducible [19]. Adequate precision compares the range of the predicted values at the design points to the average prediction error and a ratio greater than 4 is desirable [20]. The coefficient of determination (R^2) evaluates the correlation between the experimental data and the predicted responses quantitatively. It is known that R^2 always increases on adding terms to the model, whereas, the adjusted R^2 does not. In fact if unnecessary terms are added, the value of adjusted R^2 often decreases [20]. Here, the adjusted R^2 value (0.8) was smaller than R^2 (0.86). In addition to the regression coefficient, the adequacy of the model was also evaluated by the residuals (difference between the observed and predicted response value).

The actual and the predicted degradation percent are shown in Fig. 7. It is observed that there are tendencies in the linear regression fit, and the model explains the experimental range studied sufficiently. Also, Fig. 8 is the normal percent probability plot of the residues that shows an approximate linearity confirming normality of the data.

4.3. Effect of variables as response surface and counter plots

In order to attain a better understanding of the effects of the independent parameters and their interactions on the response, 3D plots for the degrada-

Table 3
ANOVA for response surface reduced quadratic model

Source	Sum of squares	Degree of freedom	Mean square	F-value	p-value	
Model	2046.91	8	255.86	15.72	< 0.0001	Significant
X_1	433.93	1	433.93	26.66	< 0.0001	
X_2	269.01	1	269.01	16.53	0.0006	
X_3	29.82	1	29.82	1.83	0.1903	
X_4	241.20	1	241.20	14.82	0.0009	
X_1^2	80.66	1	80.66	4.95	0.0371	
X_2^2	102.84	1	102.84	6.32	0.0202	
X_3^2	74.83	1	74.83	4.60	0.0439	
X_4^2	475.56	1	475.56	29.21	< 0.0001	
Residual	341.85	21	16.28			
Lack of fit	313.63	16	19.60	3.47	0.0872	Not significant
Pure error	28.21	5	5.64			
Cor. total	2388.75	29				

$R^2 = 0.86$, R^2adj $= 0.80$, C.V.% $= 7.20$, adequate precision $= 19.51$.
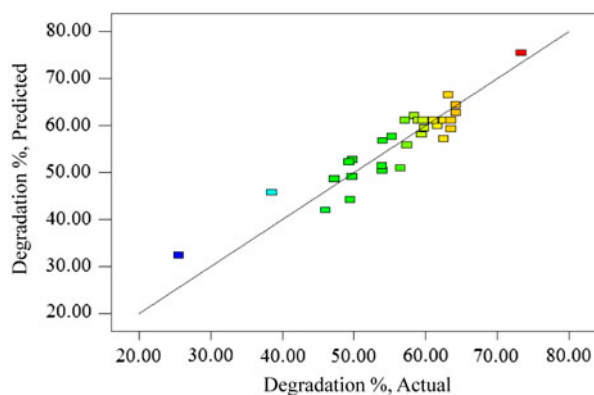
Fig. 7. The actual and predicted degradation percent of naphthalene.
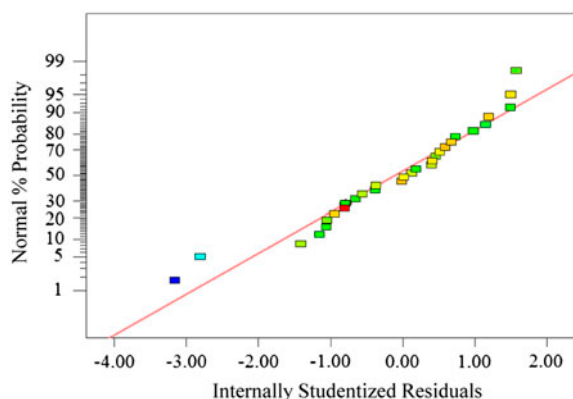
Fig. 8. The studentized residual and normal percent probability plot.

tion percent were presented based on the proposed model (Eq. (3)). The chemical naphthalene degradation percent was defined as follows:

$$\text{Degradation } \% = \frac{C_0 - C_F}{C_0} \times 100 \qquad (4)$$

where C_0 is the initial concentration of naphthalene and C_F is the final naphthalene concentration. In Fig. 9, the effect of agitation speed and air flow rate on degradation percent have been shown, whereas TiO$_2$ concentration and UV light intensity are equal to 2 g/L and 16 W, respectively.

The graphic analysis shows that agitation speed, varying from 50 to 150 rpm, has a positive effect on degradation. This behavior can be attribiuted to the enhancement of mass transfer coefficient (k_C) with agitation speed. Considering the spherical TiO$_2$ nano-particles suspended in the solution, equation related to k_C is like equation as follows [21]:

$$k_C = 0.6 \left(\frac{D_{AB}^{0.67}}{v^{0.17}} \right) \left(\frac{U}{d_p} \right)^{0.5} \qquad (5)$$

where D_{AB} is the diffusion coefficient of the naphtha-lene in water, d_p is the nanoparticle diameter, v is the kinematic viscosity of water, and U is the velocity of the fluid passing from the spherical particle. Consider-ing Eq. (5), there are two ways to increase k_C. First, reducing d_p and second increasing U. By enhancing the agitation speed, U will increase, so k_C enhances.

On the other hand, it is evident that naphthalene degradation percent increases with air flow rate especially in the range of 3–5 L/h. This enhancement

can occur due to the increasing concentration of oxygen in the solution as an electron scavenger, as other researchers mentioned in their studies [1,22]. However, With more precision in Fig. 9(a), it seems that at the values close to X_1 = 150 rpm and X_2 = 5.0 L/h, the graph becomes more smooth and it can be postulated that the agitation speed and air flow rate have no significant interaction effect at agitation speeds higher than 150 rpm.

Also, in Fig. 10 the effect of TiO_2 loading and UV light intensity on degradation percent have been shown, whereas agitation speed and air flow rate are equal to 100 rpm and 4 L/h, respectively.

As shown in Fig. 10, TiO_2 loading varied from 1.5 to 2.5 g/L has low influence on the degradation percent. However, catalyst loading showed an optimum amount equal to 2.17 g/L at mentioned range. This can be rationalized in terms of the availability of active sites on TiO_2 surface and the penetration of activating light into the suspension. The availability of the active sites increases with the catalyst concentration in the suspension, but the light penetration decreases with the catalyst concentration in the suspension due to the "screening effect" and opacity of the suspension [14,15,23].

Such as was the case before, UV light power intensity showed an optimum value equal to 18.69 W to achieve maximum naphthalene degradation percent. These results are quite consistent with other research results. Ollis et al. [24] expressed that at low UV light intensities, the reaction rate has a linear relation with the light intensity; at moderate light intensities beyond a certain value, the reaction rate depends on the square root of the light intensity; and at high light intensities, the light intensity has little negative effect on the reaction rate.

4.4. Determination of optimal conditions for degradation of naphthalene

In optimization, the degradation percent was maximized to 70% for 20 mg/L of initial naphthalene concentration. The optimum value of operational parameteres has been shown in Table 4 for 170 min of
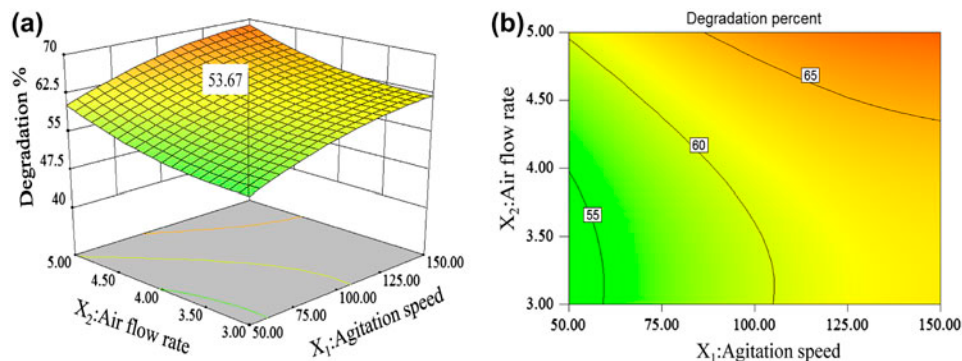
Fig. 9. Response surface plot (a) and contour lines plot (b) indicating the effect of agitation speed and air flow rate upon the degradation percent of naphthalene, under the condition of X_3 = 2 g/L and X_4 = 16 W.
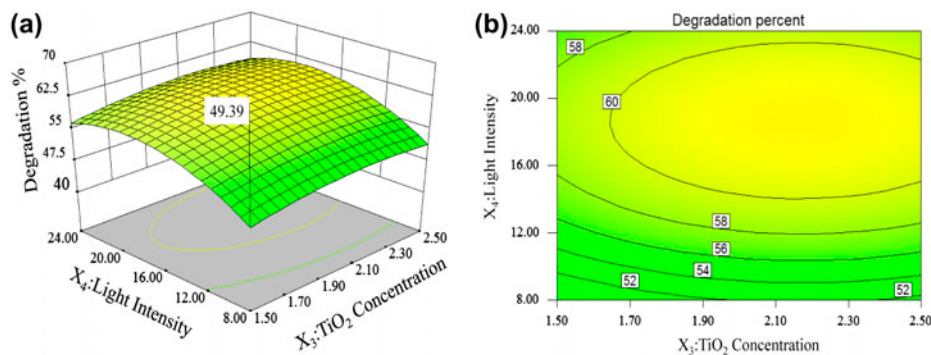
Fig. 10. 3D surface graph (a) and 2D contour plot (b) indicating the effect of photocatalyst loading and light intensity for naphthalene degradation percent, under the condition of X_1 = 100 rpm and X_2 = 4 L/h.

Table 4
Result of confirmation experiments for optimum conditions

| Parameter | Optimum value | Degradation percent (%) | |
		Predictive	Experimental
X_1 (rpm)	150.00	69.04[*]	66.30[*]
X_2 (L/h)	5.00	69.64[**]	
X_3 (g/L)	2.17		

[*]X_4 = 16 W.
[**]X_4 = 18.67.

treatment time with the desirability value of 0.922. Also, to confirm the model adequacy, the model was validated by carrying out experiments using the optimum conditions.

Three replicative experiments were carried out in the reactor which yielded an average maximum naphthalene degradation rate equal to 66.3%. However, due to the operational limitations in experiments that were carried out at optimum conditions, the value of UV light intensity was regulated to 16 W. Also, in order to make a better comparison, the predicted value of degradation efficiency for light intensity of 16 W was added to Table 4. The good agreement between the predictive and experimental results verified the validity of obtained optimal point.

Conclusions

In this paper, the photocatalytic degradation of naphthalene in TiO_2/UV system was analyzed by the use of RSM. The CCD was applied by considering the agitation speed (X_1), air flow rate (X_2), photocatalyst loading (X_3), and UV light intensity (X_4). The results showed that at the first-order (linear term) state, the agitation speed is the most significant parameter on the naphthalene degradation.

Analysis of variance showed an appropriate coefficient of determination ($R^2 = 0.86$ and $R^2adj = 0.8$), thus assure a sufficient adaption of the second-order regression model with the experimental data. Also, the optimum values of X_1, X_2, X_3, and X_4 were 150 rpm, 5 L/h, 2.17 g/L, 18.67 W, respectively. At optimum conditions, the degradation percent was maximized to about 70% for 20 mg/L of initial naphthalene concentration.

According to these results, the photocatalytic process can be an appropriate alternative to the conventional methods for the optimum refining process of organic wastewater at low concentrations.

Symbols

CV	—	coefficient of variance
C	—	concentration at any time, mg/L
C_0	—	initial concentration, mg/L
C_F	—	final concentration, mg/L
d_P	—	nanoparticle diameter, m
D_{AB}	—	diffusion coefficient, m^2/s
e	—	random error
k	—	number of factors
k_C	—	mass transfer coefficient, mg/(L min)
R^2	—	coefficient of determination
R^2adj	—	adjusted coefficient of determination
U	—	velocity of the fluid passing from the spherical particle, m/s
x_i, x_j	—	coded values
X_0	—	value of variable at the center point
X_i	—	value of the independent variable
Y	—	response variable
β_0	—	constant coefficient
β_i	—	linear coefficients
β_{ii}	—	quadratic coefficient
β_{ij}	—	interaction coefficients
v	—	cinematic viscosity, kg/(m s)
Δx	—	step change value

References

[1] M.J. Garcia Martinez, L. Canoira, G. Blazquez, I. Da Riva, R. Alcantara, J.F. Llamas, Continuous photodegradation of naphthalene in water catalyzed by TiO_2 supported on glass Raschig rings, Chem. Eng. J. 110 (2005) 123–128.
[2] Y.H. Shen, T.H. Chaung, Removal of dissolved organic carbon by coagulation and adsorption from polluted source water in southern taiwan, Environ. Int. 24 (1998) 497–503.
[3] A. Maartens, P. Swart, E.P. Jacobs, Removal of natural organic matter by ultrafiltration: Characterisation, fouling and cleaning, Water Sci. Technol. 40 (1999) 113–120.
[4] A.I. Schafer, A. Pihlajamaki, A.G. Fane, T.D. Waite, M. Nystrom, Natural organic matter removal by nanofiltration: Effects of solution chemistry on retention of low molar mass acids vs. bulk organic matter, J. Membr. Sci. 242 (2004) 73–85.
[5] K. Maillacheruvu, S. Safaai, Naphthalene removal from aqueous systems by *Sagittarius sp*, J. Environ. Sci. Health, A37 (2002) 845–861.
[6] M.N. Chong, B. Jin, C.W.K. Chow, C. Saint, Recent developments in photocatalytic water treatment technology: A review, Water Res. 44 (2010) 2997–3027.

[7] L. Ming Chun, R. Gwo Dong, C.H. Jong Nan, C.P. Huang, Photocatalytic mineralization of toxic chemicals with illuminated TiO_2, Chem. Eng. Commun. 139 (1995) 1–13.

[8] S.K. Wen, Photocatalytic oxidation of pesticide rinsate, J. Environ. Sci. Health, B37 (2002) 65–74.

[9] J. Dostanic, D. Loncarevic, L. Rozic, S. Petrovic, D. Mijin, D.M. Jovanovic, Photocatalytic degradation of azo pyridone dye: Optimization using response surface methodology, Desalin. Water Treat. 51 (2013) 2802–2812.

[10] B. Shahmoradi, I.A. Ibrahim, N. Sakamoto, S. Ananda, R. Somashekar, T.N. Guru Row, K. Byrappa, Photocatalytic treatment of municipal wastewater using modified neodymium doped TiO_2 hybrid nanoparticles, J. Environ. Sci. Health, A45 (2010) 1248–1255.

[11] J. Theurich, D.W. Bahnemann, Photocatalytic degradation of naphthalene and anthracene: GC-MS analysis of the degradation pathway, Res. Chem. lntermed. 23 (1997) 247–274.

[12] T. Onho, K. Tokieda, S. Higashida, M. Matsumura, Synergism between rutile and anatase TiO_2 particles in photocatalytic oxidation of naphthalene, Appl. Catal. A-Gen. 244 (2003) 383–391.

[13] A. Lair, C. Ferronato, J. Chovelon, J.M. Herrmann, Naphthalene degradation in water by heterogeneous photocatalysis: An investigation of the influence of inorganic anions, J. Photochem. Photobiol., A. 193 (2008) 193–203.

[14] M. Montazerozohori, S.M. Jahromi, Photocatalytic decolorization of ethyl orange at various buffer solutions using nano-titanium dioxide: a kinetic investigation, Desalin. Water Treat. 48 (2012) 261–266.

[15] C.H. Wu, H.W. Chang, J.M. Chern, Basic dye decomposition kinetics in a photocatalytic slurry reactor, J. Hazard. Mater. 137 (2006) 336–343.

[16] M.C. Marti Calatayud, M.C. Vincent Vela, S.A. Blanco J.L. Garcia, E.B. Rodriguez, Analysis and optimization of the influence of operating conditions in the ultrafiltration of macromolecules using a response surface methodological approach, Chem. Eng. J. 156 (2010) 337–346.

[17] M. Khayet, C. Cojocaru, G. Zakrzewska, Trznadel, Response surface modeling and optimization in pervaporation, J. Membr. Sci. 321 (2008) 272–283.

[18] C. Cojocaru, G.Z. Trznadel, Response surface modeling and optimization of copper removal from aqua solutions using polymer assisted ultrafiltration, J. Membr. Sci. 298 (2007) 56–70.

[19] Sh Ghafari, H. Abdul Aziz, M.H. Isa, A.A. Zinatizadeh, Application of response surface methodology (RSM) to optimize coagulation–flocculation treatment of leachate using poly-aluminum chloride (PAC) and alum, J. Hazard. Mater. 163 (2009) 650–656.

[20] M.Y. Noordin, V.C. Venkatesh, S. Sharif, S. Elting, A. Abdullah, Application of response surface methodology in describing the performance of coated carbide tools when turning AISI 1045 steel, J. Mater. Process. Technol. 145 (2004) 46–58.

[21] H.S. Fogler, Elements of Chemical Reaction Engineering. Prentice-Hall of India, Delhi, 2004.

[22] A.R. Khataee, M. Zarei, M. Fathinia, MKh Jafari, Photocatalytic degradation of an anthraquinone dye on immobilized TiO_2 nanoparticles in a rectangular reactor: Destruction pathway and response surface approach, Desalination 268 (2011) 126–133.

[23] A.H. Mahvi, M. Ghanbarian, S. Nasseri, A. Khairi, Mineralization and discoloration of textile wastewater by TiO_2 nanoparticles, Desalination 239 (2009) 309–316.

[24] D.F. Ollis, E. Pelizzetty, N. Serpone, Photocatalyzed destruction of water contaminants, Environ. Sci. Technol. 25 (1991) 1522–1529.